www.czasopisma.pan.pl PAN www.journals.pan.pl

POLISH POLAR RESEARCH
vol. 39, no. 4, pp. 457–480, 2018 doi: 10.24425/118756

Effects of recent cooling in the Antarctic Peninsula on snow density and surface mass balance

Cayetana RECIO-BLITZ[1], Francisco J. NAVARRO[1], Jaime OTERO[1], Javier LAPAZARAN[1] and Sergi GONZALEZ[2]

[1] *Department of Mathematics Applied to ICT, Universidad Politécnica de Madrid, Spain*

[2] *AEMET Antarctic Group, Spanish Meteorological Service (AEMET), Spain*

<cayetana.rblitz@upm.es> <francisco.navarro@upm.es> <jaime.otero@upm.es> <javier.lapazaran@upm.es> <sgonzalezh@aemet.es>

Abstract: The Antarctic Peninsula region has experienced a recent cooling for about 15 years since the beginning of the 21st century. In Livingston Island, this cooling has been of 0.8°C over the 12-yr period 2004–2016, and of 1.0°C for the summer average temperatures over the same period. In this paper, we analyse whether this observed cooling has implied a significant change in the density of the snowpack covering Hurd and Johnsons glaciers, and whether such a density change has had, by itself, a noticeable impact in the calculated surface mass balance. Our results indicate a decrease in the snow density by 22 kg m^{-3} over the study period. The density changes are shown to be correlated with the summer temperature changes. We show that this observed decrease in density does not have an appreciable effect on the calculated surface mass balance, as the corresponding changes are below the usual error range of the surface mass balance estimates. This relieves us from the need of detailed and time-consuming snow density measurements at every mass-balance campaign.

Key words: Antarctica, Livingston Island, glacier snow cover, compaction, air temperature.

Introduction

Glaciers and ice caps (henceforth glaciers) all across the globe have a total ice volume of roughly 1% that of the combined volume of the Greenland and Antarctic ice sheets. Yet, the current estimated contribution to sea-level rise (SLR) from wastage from glaciers is larger than that of the ice sheets. The estimated contributions over the period 1993–2010 are of 27% and 21%, respectively (Stocker *et al.* 2013). All glacier regions currently show a negative

mass budget, *i.e.* a net mass loss (Gardner *et al.* 2013). As the glaciers lose mass at an accelerated path, their contribution to SLR could be surpassed by that of the ice sheets. The quantification of the current and the projected mass balance of glaciers, by both observations and modelling, is therefore crucial to understanding the present and future contributions to SLR from melting of land ice. At the global scale, the most important contributor to the mass losses is surface ablation, which accounts for ~90% of the current losses, the remaining 10% corresponding to frontal ablation, *i.e.* the combination of calving and submarine and subaerial melting at the glacier front of marine-terminating glaciers (Cogley *et al.* 2011). Projected frontal ablation rates increase over the next decades, but then are gradually reduced as marine terminating glaciers retreat onto land (Huss and Hock 2015), which stresses the importance of the study of the surface mass balance (SMB) of glaciers.

The calculation of the observed mass balance of glaciers can be accomplished using a variety of methods (*e.g.* Hagen and Reeh 2004; Bamber and Kwok 2004; Cuffey and Paterson 2010; Hanna *et al.* 2013). Among the most usual methods, the gravimetric method is the only one that directly estimates mass changes. All other common methods (*e.g.* glaciological, geodetic/altimetric) yield volume changes and thus require a conversion from volume to mass, using density. Among these methods, the glaciological method (Østrem and Brugman 1991), readily provides both winter and summer SMBs. Having this separation of the annual SMB is important to understanding the reasons of the observed changes. For instance, whether an observed decrease in annual mass balance has been due to decreased accumulation or increased melt, or both, or whether an increased accumulation partially offsets an increased melt. In the glaciological method, the density of snow, measured at snow pits, plays a crucial role. It is used to calculate the winter balance from stake readings, snow probing and snow pits. It is also used, together with the ice density, to calculate the summer balance from stake readings. In the geodetic method by digital elevation model (DEM) differencing, as well as in the repeat altimetry (*e.g.* ICESat) method, potential changes in firn thickness and density between the surveys are needed. However, often Sorge's Law (Bader 1954) is assumed, *i.e.* that there is no changing firn thickness or density through time and that all volume changes are of glacier ice, in which case, snow and firn densities do not play a role.

The glaciological method for calculating surface mass balance is used not only for individual glaciers, but extrapolation from local SMB studies to estimate regional balances has been a common practice in the past and is still currently used in regions where estimates with other wider-scale techniques are not available (Gardner *et al.* 2013). Though the glaciological method is especially suited for small glaciers, we note that model projections indicate that, over the next decade, 28% of the sea-level rise contribution may originate from glaciers that are smaller than 10 km^2 at the present time (Huss and Hock

www.czasopisma.pan.pl PAN www.journals.pan.pl

2015). Moreover, the World Glacier Monitoring Service (http://wgms.ch/) holds an extensive collection of time series of SMB observations made using the glaciological method for many glaciers from different regions and, in many cases, covering several decades. These facts reinforce the importance of the glaciological method, in which knowledge of the snow density plays an important role.

Under warming climate, it can be expected that snow density will increase, because of increased surface melt and percolation, with subsequent refreezing within the snowpack. However, not all glaciated regions are currently warming. For instance, the Antarctic Peninsula region, which during the second half of the 20th century was among the most rapidly warming regions on Earth (Turner *et al.* 2005), has experienced since the start of the 21st century a period of sustained cooling for about 15 years (Turner *et al.* 2016). Moreover, this recent cooling has been shown to have had some observable effects on the regional cryosphere, including a longer duration of the snow cover, a shift from negative to predominantly positive SMBs and a shift from thickening to thinning of the active layer of permafrost in certain areas of the periphery of the northern Antarctic Peninsula and the South Shetland Islands (Oliva *et al.* 2017). Consequently, it can be expected that the density of the snowpack may decrease under these cooling conditions. Here, we set out to test if this relatively short period of sustained cooling has been enough to produce a measurable decrease in the density of the snowpack covering the regional glaciers and to verify whether this expected decrease in density is sufficient to have a significant effect on SMB calculations. The latter issue has practical implications, as, if a significant decrease in density does not imply a corresponding significant decrease in the calculated SMB, then time-consuming density measurements do not have to be made during each field campaign.

We focus here on changes in the calculated SMB due to the density changes alone. Clearly, regional climate changes have an impact on the SMB, both through changes in snow precipitation and in melting rates of snow and ice. In fact, as mentioned, the recent regional cooling in the northern Antarctic Peninsula has implied a shift to predominantly positive SMBs, which has been attributed to both increased snow accumulation and decreased melt (Navarro *et al.* 2013). The glaciers in this region has been shown to be extremely sensitive to temperature changes. Mass-balance modelling by Jonsell *et al.* (2012) showed that a temperature increase of 0.5°C resulted in melting rates increasing by 56%. This high sensitivity of SMB to temperature changes has been attributed to the fact that the summer average temperatures of these glaciers is very close to the melting point (0°C), so a small change in temperature implies a shift from non-melting to melting conditions, or vice versa.

The experiments designed to address the two above scientific issues were carried out using data from two glaciers on Livingston Island, West Antarctica, for which we had sufficient glaciological and meteorological data. We used these

data to first analyse the temporal evolution of snow density, temperature and positive degree days (PDDs), then we analysed the temporal correlation among them, and finally we explored the possible influence of the observed density changes on the calculated surface mass balance. Although the calculation of the latter for the winter balance is trivial, in the case of the summer balance it is not known in advance how much of the total melt results from melting snow, and how much from melting ice. Moreover, using a decreased density in the winter balance calculation implies a less positive winter balance, while the use of decreased density in the summer balance calculation renders a less negative summer balance, so both effects could partly balance each other. This justifies the detailed analysis undertaken in this paper.

Study area and data

Study area. — Our study area is the Hurd Peninsula (62°39' – 62°42'S, 60°19' – 60°25'W), settled on Livingston Island, South Shetland Islands archipelago, West Antarctica, where the Spanish Antarctic Station Juan Carlos I (JCI) Station is located (Fig. 1). Hurd Peninsula is covered by an ice cap extending over an area of about 13.5 km^2 and spans an altitude range from 0 to 370 m a.s.l. This ice cap is divided into several glacial basins. Our study focuses on the two main basins. The first one is Johnsons Glacier, a tidewater glacier, which flows mainly to the northwest, ending on a glacier front of 50 m in height extending 500–600 m along the coast. The second one is Hurd Glacier, which flows mainly to the southwest and ends on land. It has three major lobes: Sally Rocks, Las Palmas and Argentina. The ice divide that separates Hurd and Johnsons is between 250 and 330 m a.s.l. Hurd Glacier has an average surface slope of approximately 3°, while its western-flowing lobes, Argentina and Las Palmas, have much steeper slopes. The typical slopes of Johnsons Glacier vary between 10° in the north and 6° in the south. The ice cap of the Hurd Peninsula is a polythermal ice mass, with a top layer of cold ice, several tens of metres thick, on the ablation zone. This layer is uniformly distributed on Hurd's ablation zone but shows a more irregular distribution in Johnsons' ablation zone (Navarro *et al.* 2009).

Hurd Peninsula is subject to the maritime climate of the western region of the Antarctic Peninsula. The annual average temperature at the Spanish Antarctic Station Juan Carlos I during the period 1994–2014 was -1.2°C, with average summer (December–January–February) and winter (June–July–August) temperatures of 1.9 and -4.7°C, respectively (Bañón and Vasallo 2015).

Hurd and Johnsons, together with Glaciar Bahía del Diablo in Vega Island, are the only glaciers in the Antarctic Peninsula region with 15 or more years of SMB series in the World Glacier Monitoring Service database (WGMS,

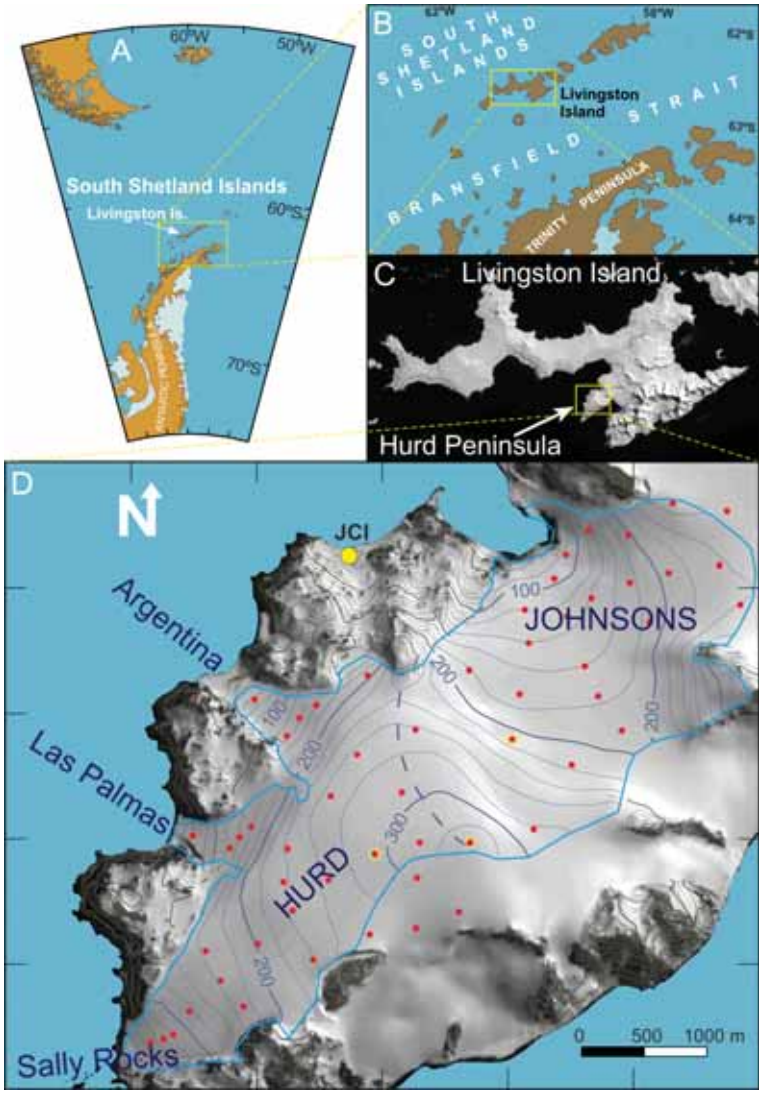

Fig. 1. Location of the South Shetland Islands archipelago (**A**), Livingston Island (**B**) and Hurd Peninsula (**C**); Copernicus Sentinel image of 2013. Map **D** shows surface elevation of Hurd and Johnsons glaciers and location of the mass balance stakes in 2015–16 (red dots), snow pits (yellow-circled red dots) and the automatic weather station at Juan Carlos I Station (JCI, yellow dot). The continuous blue line represents the glacier limits and the dashed blue line indicates the location of the ice divide separating Hurd and Johnsons glaciers. The glaciated zone on the southeast of Hurd Peninsula shown in the figure without contour lines corresponds to other glacier basins which flow to the southeast and are not addressed by this study. Four of the stakes shown in the figure are located in this zone, and thus outside of our study area. We left them in this figure because their values were used to interpolate (rather than extrapolate) the SMB values of Hurd Glacier in its part adjacent to the location of these stakes. The area shown in panel D corresponds to the UTM coordinates (sheet 20E) 631000–637000 (easting) and 3045000–3050000 (northing). The distance between tick marks is of 1 km.

http://wgms.ch). The annual SMB of these glaciers shows a large interannual variability, with recorded extreme values of -0.86 and 0.75 m w.e., although these time series show consistently positive SMBs since 2010 compared with predominantly negative SMBs in the previous decade (Ximenis *et al.* 1999; Ximenis 2001; Navarro *et al.* 2013). The average SMB over the hydrological years 2002–2016 has been of -0.02 and 0.19 m w.e. for Hurd and Johnsons Glacier, respectively (unpublished data from the authors). We note that the hydrological years considered here are those of the southern hemisphere, so that *e.g.* year 2002 spans the period 1 April 2001–31 March 2002 (Cogley *et al.* 2011). The slightly lower SMB for Hurd as compared with Johnsons is due to (i) its lower accumulation rates, favoured by the snow redistribution by wind, and (ii) its greater ablation rates due to Hurd's hypsometry, which has a larger share of area at lower elevations compared with Johnsons (Navarro *et al.* 2013). The equilibrium line altitude (ELA) over the period 2002–2016 shows a large variability, ranging between 0 and 310 m for Hurd Glacier (averaging 170 ± 107 m) and between 0 and 235 m for Johnsons Glacier (averaging 148 ± 73 m).

Data and methods

Available field data. — The main data used in this study are accumulation and ablation from stake readings and snow probing, snow density measured in snow pits, and temperature and precipitation records from an automatic weather station (AWS).

The accumulation and ablation data correspond to a network of stakes deployed by the authors on Hurd and Johnsons glaciers starting in 2000–2001 (Fig. 1). The network consists of about 50–60 stakes, which sample quite homogeneously both the accumulation an ablation areas. These stakes are measured at least twice per year, at the beginning and end of the melting season, nearly coincident with the opening and closing of the summer-only JCI station. The stake readings are complemented by measurements of the tilt and orientation of each stake, to correct the readings for stake inclination, and by probing to determine the local thickness of the snow layer. Repeated differential GPS positioning is also performed at the stakes to calculate the average velocities (summer, winter, annual).

Since 2004, we also measure snow density at different depths in snow pits. These measurements are made twice per year (at the beginning and end of each melting season). Currently, they are made at five locations in the accumulation zones of Hurd and Johnsons glaciers; however, only data for three pits are available for the entire study period (marked in Fig. 1) and therefore our analysis will be restricted to the data from these pits. These snow pits are dug to the depth of the end of the previous summer surface, typically 2 m in depth. We measure

snow density using a steel cylinder of 1 litre of volume that continuously samples the snow column, in vertical direction, providing 20-cm average densities. The estimated accuracy of each individual density measurement is of 10 kg m^{-3}. We get in this way density-versus-depth curves $\rho_w^k(H)$ and $\rho_s^k(H)$ for the end-of-winter and end-of-summer snowpacks of year *k*, which are used for the surface mass balance calculations. In each pit we also measure the depth and thickness of the ice lenses, and record some characteristics of the snow determined by visual inspection (ice crystal size, wetness), although these stratigraphic data are not relevant to the current study.

Temperature and precipitation data were obtained from an AWS located at JCI station (62.66°S 60.39°W; Fig. 1) operated by the Spanish Met Office-AEMET (Bañón and Vasallo 2015). We chose this AWS instead of another one located on-glacier because the record for the latter spans only the period Dec. 2006–Jan. 2015 for Johnsons Glacier and then was moved to Hurd Glacier. An analysis of the correlation between both AWSs can be found in Jonsell *et al*. (2012). JCI station provides year-round measurements of various meteorological and radiation variables (see in Table 1 those used in this study). These measurements started in 1988 but continuous recordings with only minor data gaps are only available since 2005, one year later than the start of the snow density measurements. Unfortunately, only total precipitation was recorded, so we had no means of distinguishing between solid and liquid precipitation, which undermined our analysis of the possible influence of liquid precipitation changes on density variations. Under ideal conditions, the partitioning between solid and liquid precipitation could be approximated using air temperature. However, in our case study we refrained from doing so because JCI station was unattended for 8–9 months in a year, which has a negative impact on the quality of the precipitation records. Moreover, the station is located close to sea level, while Hurd and Johnsons glaciers span an altitude range from 0 to 370 m a.s.l., so precipitation could be liquid at JCI, but solid on part of the glacier. Extrapolation to the glacier of JCI station temperatures, using lapse rates, would make the partitioning between solid and liquid precipitation even more uncertain.

Table 1

Meteorological variables measured at Juan Carlos I Station used in this study, with indication of sensor, range and accuracy.

Variable	Sensor	Range	Accuracy
Temperature	Vaisala HMP45C	-40°C to +60°C	± 0.2°C to ± 0.4°C
Relative humidity	Vaisala HMP45C	0% to 100%	± 2% to ± 3%
Precipitation	RM Young 52203	n/a	± 2% to ± 3%

We also used temperature data collected in Bellingshausen Station, located in the neighbouring King George Island. These data were retrieved from the Reader database (BAS 2018).

Our temperature data was recorded at JCI station, close to sea level. To calculate the positive degree day sum (PDD), *i.e.* the sum of mean daily temperature for all days where the temperature is above 0°C, as a value appropriate to our study glaciers, we did as follows. We decreased the temperature values recorded at JCI by an amount equal to the product of the measured temperature lapse rate and an 'average' altitude of our glaciers. We took such an average as the altitude at which there are equal amounts of glacier surface area above and below it (*i.e.* a hypsometric average altitude).

Temporal evolution of density. — In what follows, as to winter, we will refer to the extended winter comprising autumn, winter and spring, *i.e.* the period excluding the summer season. The densities measured at the end of winter are representative of the integrated glacier conditions along the entire winter, while those measured at the end of summer are representative of the integrated glacier conditions along the whole year (not only the summer). Consequently, end-of-winter densities should be compared against winter-averaged temperatures or winter PDDs, but end-of-summer densities should be compared with annually-averaged temperatures or annual PDDs. The density changes from end of summer to end of winter can be compared with summer-averaged temperatures or summer PDDs. With the available data, we carried out an analysis of the temporal evolution of the winter-averaged and annually-averaged snow density to detect possible trends over the 12-year period 2004–2016. With this aim, we first calculated, for each pit measured at the end of winter of a given year, the vertically-averaged density at each pit, and then we calculated the mean of these density values for the year under consideration. We obtained in this way a time series of end-of-winter averaged densities, $\rho_w(t)$. We proceeded similarly with the pits measured at the end of each year's summer, obtaining a time series of end-of-summer averaged densities, $\rho_s(t)$. Note that, although we refer to them as "summer", they are values representing the entire year. The time-averaged values (over the period 2004–2016) of $\rho_w(t)$ and $\rho_s(t)$ will be denoted by $\bar{\rho}_w$ and $\bar{\rho}_s$, respectively. We took the standard error of the mean, $e = \sigma/\sqrt{N}$, with σ the standard deviation and N the number of measurements, as error of the yearly averages of density. This is the quantity shown as error bar in our density-versus-time plots. This density averaging was followed by a least-squares fit to a straight line of the time series of end-of-winter and end-of-summer averaged densities, which we will denote as $\hat{\rho}_w(t)$ and $\hat{\rho}_s(t)$. We denote with $\hat{\rho}_w^{\text{init}}$ and $\hat{\rho}_s^{\text{init}}$ the density value for $t = 0$ of the straight-line fits $\hat{\rho}_w(t)$ and $\hat{\rho}_s(t)$, respectively (see Fig. 3). For each linear fit, we calculated the coefficient of determination R^2 and the root-mean-square error (RMSE) of the fit. We also computed the p-value

of the linear fit, to determine whether we can safely reject the null hypothesis that there is no trend. In this study, following common practice, we considered the linear trends to be statistically significant if $p < 0.05$. Additionally, we considered the trend as weakly significant if $0.05 \leq p < 0.1$, poorly significant if $0.01 \leq p < 0.15$ and nonsignificant if $p \geq 0.15$.

Temporal evolution of temperature and positive-degree days (PDDs). — Temperature data from 2005 to 2016 were processed using the methodology described in Gonzalez *et al.* (2018). In short, daily 10-minute readings were averaged, rejecting days with less than 80% measurements available. Thereafter, data gaps were filled-in and the daily series were homogenized applying a software tool developed by Guijarro (2017), using AWS data from Gabriel de Castilla Station (GdC, 62.98°S 60.68°W), in the neighbouring Deception Island, and the four nearest ERA Interim reanalysis grid points. It has been observed that JCI station data are sensitive to the synoptic conditions over the Antarctic Peninsula (Gonzalez *et al.* 2018).

Based on the processed daily temperature data, we calculated extended winter (autumn, winter and spring), summer and annual averages to analyse their time evolution, with trends given by the slopes of associated linear fits. We also analysed separately the entire time series of daily temperatures, covering 11 years, to detect possible trends. In this case, we fit the temperature data to a function combining a linear trend and a sinusoidal oscillation with annual periodicity that accounts for seasonality, as follows:

$$T = mt + n + A \sin\left(\frac{2\pi}{365.2425} t + \varphi\right), \quad (1)$$

where T is the temperature in °C, t is the time expressed in days since a reference starting time, m and n are the slope and intercept of the straight-line regression (m giving the slope of the linear trend), and A and φ are the amplitude and phase of the sinusoidal wave. The denominator 365.2425 includes allowance for leap years.

Finally, we analysed the consistency of our average temperatures (winter, summer, annual) with those calculated using data from the neighbouring Bellingshausen Station in King George Island, retrieved from the Reader database (BAS 2018). We also checked the consistency of our trends with those calculated by Oliva *et al.* (2017) using data from Bellingshausen Station.

From the daily average temperature data, we also calculated the number of days with temperature above zero and the PDDs, distinguishing between extended winter and summer values, and analysed their time evolution. PDDs are expected to be more relevant than temperatures in terms of surface melting and associated snow density changes upon refreezing.

Density versus temperature and PDDs. — Once we analysed separately the time evolution of density, PDDs and temperature, we examined the temporal correlation between snow density and temperature and PDDs (winter, summer, annual) over the 12-year study period, in the case of temperatures and PDDs.

Mass balance. — We calculated the SMB using the glaciological method (Cogley *et al.* 2011). Based on the accumulation and ablation data collected at the network of stakes, the snow thickness data from snow probing and the density data measured at the snow pits, we calculate point SMB for winter, summer, and entire years. The density-versus-depth curve $\rho_w^k(H)$ of the end-of-winter snowpack is used, together with the snow depth, to calculate the point winter balance b_w (in m in water equivalent, m w.e.). In turn, the curve $\rho_s^k(H)$ of the end-of-summer snowpack is used, together with the ice density, for which we assume 900 kg m^{-3}, to calculate the point summer balance b_s from the stake readings at the end of the summer. The point annual balance b_a is then calculated as $b_a = b_w + b_s$ (where b_s is a negative quantity, representing mass losses). We note that, because JCI station operates only during the austral summer, station closing may occur before the actual end of the melting season. For this reason, a correction is applied to b_s to account for the melting after station closing. For a given balance year, this melting correction is quantified as the discrepancy between the snow depth at the end of the subsequent winter and the difference in stake height from the measurements done at station closing time and at the beginning of the next field season, *i.e.* the start of the subsequent balance year. The point SMBs are interpolated over the glacier surface into a 25 m resolution grid using a kriging routine. These point values are then integrated over the glacier area by summing over all grid cells. This produces glacier-wide winter (B_w), summer (B_s) and annual (B_a) SMBs for the ensemble Hurd-Johnsons for each year within our study period. See more detail in Navarro *et al.* (2013). The estimated accuracy in the calculated SMBs is of ± 0.2 m w.e. (Dyurgerov 2002).

Effects of density variations on the calculated surface mass balance. — Our aim here was to verify if the snow density changes expected to occur under a cooling scenario, as observed recently in the Antarctic Peninsula region, have a significant effect on the calculated glacier-wide mass balances. With this purpose, we defined density-versus-depth profiles $\hat{\rho}_w^{\text{init}}(H)$ and $\hat{\rho}_s^{\text{init}}(H)$, for winter and summer conditions, typical of the initial warmer conditions of the start of our study period, before the initiation of the recent regional cooling. Using, for the calculation of the SMB of every year during the study period, these density profiles instead of the real ones for the year, $\rho_w^k(H)$ and $\rho_s^k(H)$, we will be able to check whether the expected snow density changes under cooler conditions have a measurable effect on the calculated SMB. We did a second experiment, in which we used, every year during the study period, constant densities $\bar{\rho}_w^{\text{init}}$

and $\bar{\rho}_s^{\text{init}}$ instead of $\hat{\rho}_w^{\text{init}}(H)$ and $\hat{\rho}_s^{\text{init}}(H)$. $\bar{\rho}_w^{\text{init}}$ and $\bar{\rho}_s^{\text{init}}$ and are simply the depth-averaged values of $\hat{\rho}_w^{\text{init}}(H)$ and $\hat{\rho}_s^{\text{init}}(H)$. The aim of this experiment was to check whether the use of depth-averaged instead of density-versus-depth density profiles implied any significant change over the first experiment.

Let us now explain how we defined the density-versus-depth profiles $\hat{\rho}_w^{\text{init}}(H)$ and $\hat{\rho}_s^{\text{init}}(H)$. Our intention was constructing density-versus-depth curves, which for simplicity we considered as straight lines, with slopes typical of end-of-winter and end-of-summer conditions. The depth-averaged values of these curves shoud be representative of the warmer conditions typical of the start of our study period. Consequently, we first calculated straight-line fits $\hat{\rho}_w(H)$ and $\hat{\rho}_s(H)$ to the data sets $\rho_w(H)$ and $\rho_s(H)$, which include, respectively, all winter and all summer density data for all years and all pits, as shown in Fig. 2. These straight lines represent average winter and summer densities for the entire study period. The p-values of the linear fits were extremely low ($p < 10^{-6}$ for the end-of-winter fit, and $p < 10^{-7}$ for the end-of-summer fit), indicating a statistically significant fit, despite the corresponding R^2 values are very low ($R^2 = 0.0869$ and $R^2 = 0.1265$, respectively). Although perhaps unexpected, this is not unusual. The coefficients estimate the trends (and the p-value its statistical significance) while R^2 represents the scatter around the regression line, and even when R^2 is low, low p-values still indicate a real relationship between the significant predictors and the response variable. But we should be aware that, because of the low R^2 values, precise predictions cannot to be expected. To make these linear fits representative of the initial warmer conditions, we shifted upwards these straight lines so that their depth-averaged values coincided with the average winter and summer densities corresponding to the start of the study period. To do this, the straight-line fits $\hat{\rho}_w(H)$ and $\hat{\rho}_s(H)$ were shifted upwards by amounts

$$\Delta\rho_w = \hat{\rho}_w^{\text{init}} - \bar{\rho}_w\,, \tag{2a}$$

$$\Delta\rho_s = \hat{\rho}_s^{\text{init}} - \bar{\rho}_s\,, \tag{2b}$$

where $\hat{\rho}_w^{\text{init}}$, $\hat{\rho}_s^{\text{init}}$, $\bar{\rho}_w$ and $\bar{\rho}_s$ have been defined in the subsection “Temporal evolution of density”. The resulting functions are

$$\hat{\rho}_w^{\text{init}}(H) = \hat{\rho}_w(H) + \Delta\rho_w = m_w H + \rho_w^0 + (\hat{\rho}_w^{\text{init}} - \bar{\rho}_w)\,, \tag{3a}$$

$$\hat{\rho}_s^{\text{init}}(H) = \hat{\rho}_s(H) + \Delta\rho_s = m_s H + \rho_s^0 + (\hat{\rho}_s^{\text{init}} - \bar{\rho}_s), \tag{3b}$$

where m_w, m_s and ρ_w^0, ρ_s^0 are the slopes and intercepts, respectively, of the straight-line fits $\hat{\rho}_w(H)$ and $\hat{\rho}_s(H)$ ($m_w = 0.00321$ kg m^{-3} m^{-1}, $m_s = 0.004428$ kg m^{-3} m^{-1}, $\rho_w^0 = 480$ kg m^{-3}, $\rho_s^0 = 502$ kg m^{-3} in our case study). The intercepts ρ_w^0 and ρ_s^0 represent the snow densities next to the glacier surface at the end of the winter and summer periods, respectively.

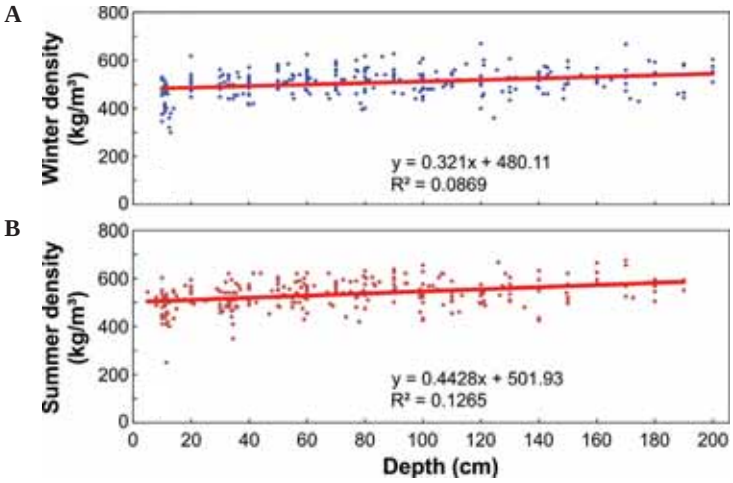

Fig. 2. Density versus depth measurements for winter (**A**) and summer (**B**), using data from all years, and corresponding straight-line fits $\hat{\rho}_w(H)$ and $\hat{\rho}_s(H)$.

Results and interpretation

Temporal evolution of density, temperature and PDDs. — The means, over the 12-year study period, of the end-of-winter- and end-of-summer averaged densities are $\bar{\rho}_w$ = 510 ± 14 kg m^{-3} and $\bar{\rho}_s$ = 523 ± 18 kg m^{-3}; the quoted errors are the standard deviations; the respective standard errors of the mean are 4 and 5 kg m^{-3}. The $\hat{\rho}_w^{\text{init}}$ and $\hat{\rho}_s^{\text{init}}$ values for the straight-line fits are 519 and 534 kg m^{-3}, respectively, producing $\Delta\rho_w$ = 9 kg m^{-3} and $\Delta\rho_s$ = 11 kg m^{-3}.

The temporal evolution of end-of-winter and end-of-summer averaged densities are shown in Fig. 3. They exhibit trends of -1.76 and -1.87 kg m^{-3} a^{-1}, which imply decreases in the density of the snow cover of -21 (winter) and -22 (summer, representing annual) kg m^{-3} over the period 2004–2016. The R^2 of the least-square fits are 0.2297 (winter) and 0.1567 (summer), the RMSEs are 12 (winter) and 16 (summer) kg m^{-3} and the p-values are 0.16 (winter) and 0.23 (summer). Although the fits are rather poor, and the trends are poorly significant (winter) and nonsignificant (summer), the winter and summer trends are consistent with each other and the fits improve slightly (to R^2 of 0.32 and 0.34 for winter and summer, respectively) if they are weighted by the inverse of the variances. We also note that the least-square linear fit to the difference $\rho_s(t) - \rho_w(t)$, which represents the change in density produced during the summer, has a slightly better coefficient of determination (R^2 = 0.32) and is more significant (p = 0.11) than the linear fits to the separate time series $\rho_w(t)$ and $\rho_s(t)$.

Regarding the behaviour of temperatures during the same period, we observe in Fig. 4 the temporal evolution of the mean winter, summer and

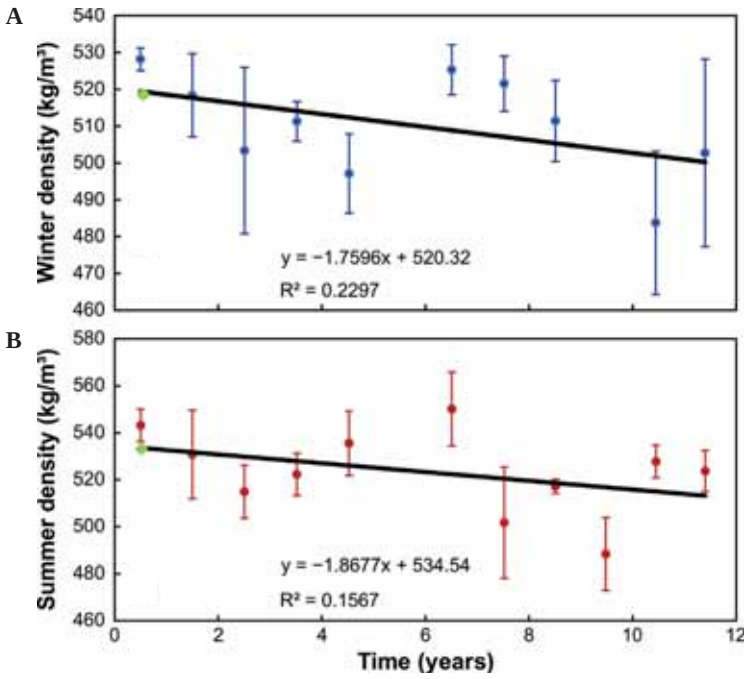

Fig. 3. Temporal evolution of the end-of-winter averaged (**A**) and end-of-summer averaged (**B**) snow density for the period 2004–2016 (time given in years counted from the start of the hydrological year 2005, *i.e.* 1 April 2004), with their linear trends illustrated by the corresponding least-square fits. The error bar for each data point is the standard error of the mean density of the year. The density data point for the hydrological year 2010 has been excluded as outlier, because the individual values making up the average for this year are inconsistent, suggesting experimental errors during fieldwork. The data point for the winter of the hydrological year 2014 is unavailable because in that year there was a single set of density measurements, at the end of the summer season. The green diamonds correspond to $\hat{\rho}_w^{\text{init}}$ and $\hat{\rho}_s^{\text{init}}$.

annual temperatures, which show linear trends of 0.031, -0.086 and -0.068°C a^{-1}. The coefficient of determination R^2 of the winter fit is very poor, of 0.0197, and its p-value is huge, of 0.68, indicating that this trend is not significant at all. The corresponding summer values (R^2 = 0.3085 and p = 0.08) are much better, while the annual values are of intermediate (but still poor) quality, with linear trend nonsignificant, because they are badly influenced by the winter values (R^2 = 0.1185 and p = 0.30). This annual trend would imply a sustained cooling of about 0.8°C in 12 years, 1.0°C in the case of summer temperatures. Although the coefficients of determination are poor, these trends are consistent with those inferred from the daily temperatures, and are also consistent with the regional trends analysed by other authors (Navarro *et al.* 2013; Oliva *et al.* 2017), as discussed later.

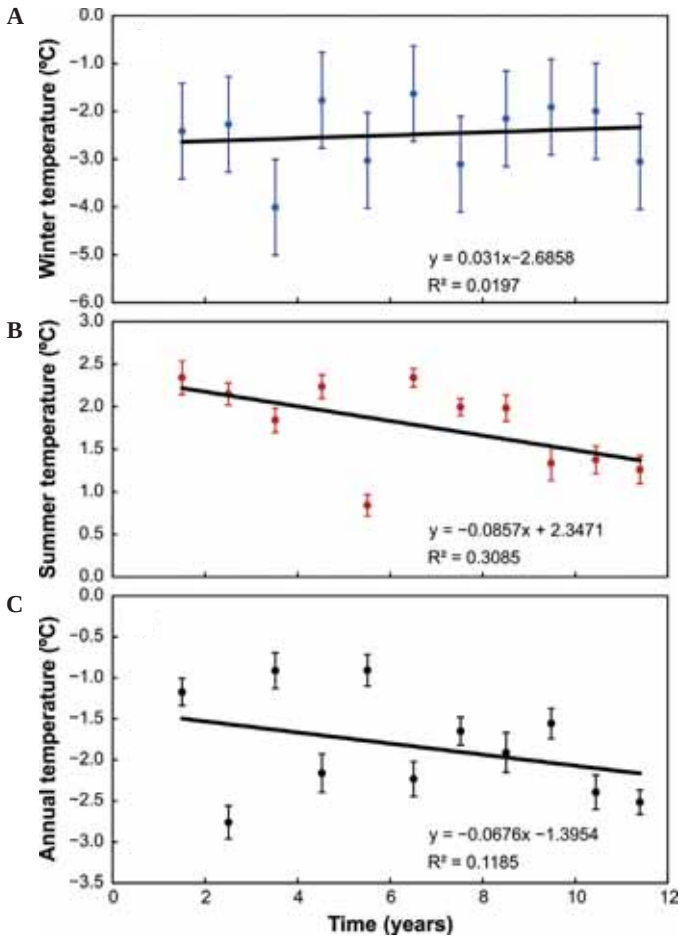

Fig. 4. Mean winter (**A**), summer (**B**) and annual (**C**) temperatures for the period 2004–2016. The error bars shown represent the instrumental error (± 0.3°C).

In Fig. 5, we show the time series of daily temperatures recorded at JCI and their least-square fit to the function given by Equation (1). There is a linear decreasing trend of -0.0001375°C d^{-1}, bracketed by (-0.0002118, -0.0000633) °C d^{-1} with a confidence interval of 95%. This is equivalent to an annual trend of -0.050°C a^{-1}, similar to the annual trend of the yearly temperature averages shown in Fig. 4C (-0.068°C a^{-1}). The least-square fit to Equation (1) has a coefficient of determination of 0.4876 and a RMSE of 2.834°C. The rather high value of the latter is due to the large interannual variability of the winter temperatures that can be observed in Fig. 5, while that of the summer temperatures is much more regular. Additionally, the extreme temperatures are much closer to the annual wave in the case of the summer temperatures as

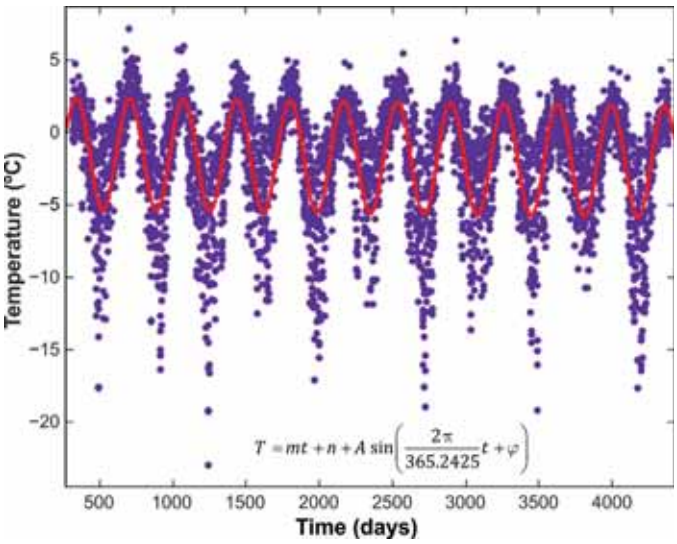

Fig. 5. Time series of daily temperatures at Juan Carlos I (purple dots) and their fit to the function given by Equation (1) (red line).

compared with the winter temperatures. The amplitude resulting from the fit is A = -3.88°C, bracketed by -4.00 and -3.76°C with a confidence interval of 95%.

This decreasing temperature trend is also consistent with the recent regional trends. Comparison with regional trends is of great interest because Hurd and Johnsons glaciers may be representative of many small glaciers, tidewater and land-terminating, respectively, in the South Shetland Islands. The analysis by Oliva *et al.* (2017) shows, for the temperature record from Bellingshausen Station in the neighbouring King George Island, an estimated trend of -0.065°C a^{-1} over the period 2006–2015, quite similar to our calculated -0.068°C a^{-1} for a nearly coincident period. We note that there is a close correlation between the temperature records of JCI and Bellingshausen Stations, illustrated in Fig. 6 for the summer average temperatures during the period 2005–2015, which has also been noted in earlier works (*e.g.* Navarro *et al.* 2013). The Pearson correlation coefficient for the summer average temperatures at both stations is 0.895. This recent cooling observed in JCI and Bellingshausen stations is highlighted in Oliva *et al.* (2017) paper as a common feature of the northern Antarctic Peninsula and the South Shetland Islands.

The winter, summer and annual PDDs show similar time evolutions as the corresponding temperatures. While the winter PDDs present a nonsignificant (R^2 = 0.0188 and p = 0.69) trend of -0.8°C a^{-1}, that for the summer PDDs is of -7.8°C a^{-1}, with an excellent and statistically significant fit (R^2 = 0.7046 and p < 0.01). The annual trend is -8.6°C a^{-1}, with R^2 = 0.5917 and p < 0.01. The total

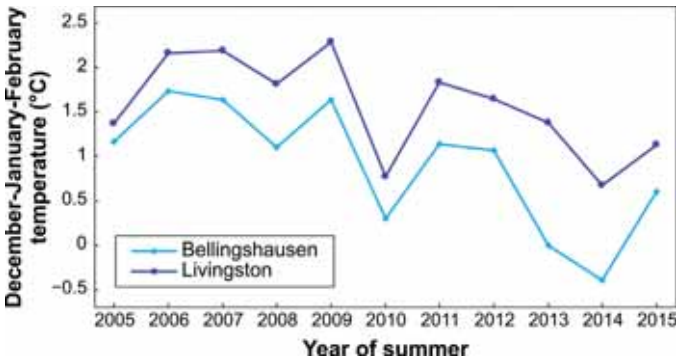

Fig. 6. Time series of summer (December–January–February) average temperatures measured at Bellingshausen and Livingston stations, illustrating their synchronous evolution. 2005 represents the summer from Dec 2004 to Feb 2005.

number of days with temperatures above zero (winter, summer, annual) follow similar patterns. The average number of days with positive temperatures, over the entire 12-yr study period, is 79, while that for the extended winter is 38, and that for the summer is 42.

There is a synchronous time evolution of summer snow density and summer and annual average temperature records and PDDs (Fig. 7), which points to a correlation of summer snow density and either summer temperature or annual temperature and PDDs, as could be expected from physical considerations. Lower surface temperatures or PDDs imply a lower amount of melting and refreezing within the snowpack, which has an expression in lower densities. Curiously, the winter density has a decreasing trend similar to that of summer density, although both the winter temperatures and PDDs show no significant changes. This suggests that perhaps other mechanisms different from surface melting and subsequent refreezing within the snowpack could be responsible for the observed decrease in density during the winter. Since the mass balance records do not indicate a decrease, but rather an increase in snow accumulation, the only likely explanation of the density decrease during winter would be a decrease in liquid winter precipitation. The effect of winter liquid precipitation on density has been observed in some northern hemisphere glaciers such as Hansbreen, in Svalbard (Grabiec *et al*. 2006). These authors noted a correlation between the densities of snow recorded at the beginning of summer and the amount of liquid precipitation during the fall-winter-spring. Unfortunately, as discussed in the available field data subsection, in the case of Livingston Island, there are no available records of liquid precipitation alone, nor an approximation of it in terms of air temperature can be safely done. Moreover, a decrease in winter liquid precipitation would be consistent with an air temperature decrease during winter, which, as mentioned, is not shown by our temperature records.

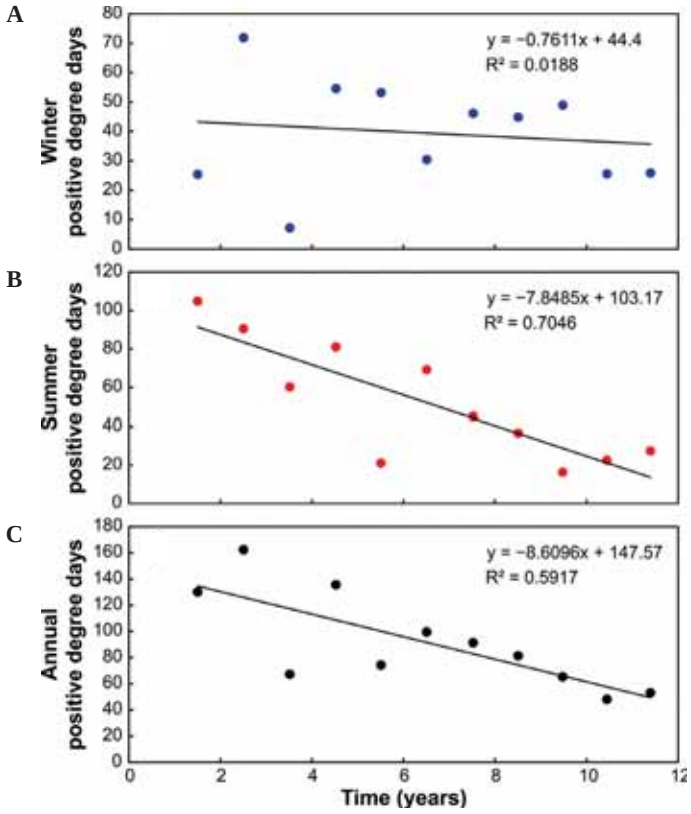

Fig. 7. Winter (**A**), summer (**B**) and annual (**C**) PDDs for the period 2004–2016.

Consequently, we cannot provide a solid evidence supporting the hypothesis that the observed decrease in density at end-of-winter density could be attributed to a decrease in winter liquid precipitation.

From a theoretical point of view, we should expect that end-of-winter densities be correlated with winter temperatures or PDDs, and end-of-summer densities be correlated with annually-averaged temperatures or PDDs over the whole year. However, in both cases, the correlations were poor, *i.e.* correlation coefficients < 0.2 for winter and < 0.3 for annual values. Only the correlation between summer densities and summer temperatures or PDDs was somehow higher (both close to 0.5), likely because most snow melting, percolation and refreezing takes place during the summer.

Effects of density variations on calculated surface mass balance. — So far, we have shown that there has been a decrease of snow density during our study period, and that this decrease in density correlates with the recent regional

cooling during the summer, which implies less snow melting, percolation and refreezing within the glacier surface snowpack. However, as discussed in the introduction, we did not know a priori whether these density changes might have a detectable effect on the calculated surface mass balance, because the magnitude of the changes could be small and, moreover, their effects on the winter and summer SMBs could partly balance each other. To ascertain this, we designed the procedure described in the methods section. The results of applying such a procedure to our accumulation and ablation data for each individual season and year over the study period are shown in Table 2 and Fig. 8. They include the winter, summer and annual balances calculated using, for each year, the snow density versus depth curves for the winter and summer of that year, together with those obtained using, for every year, the simulated density versus depth winter and summer linear fits representative of the warmer conditions typical of the start of our study period. The results for a similar density but constant in depth are also shown, *i.e.* the depth-averaged value of the simulated density versus depth linear fits for winter and summer. The table also includes the changes in calculated SMB (winter, summer, annual) of the simulated with respect to the real snow density values. Note however, that in the table we give the values of $-\Delta B$, so the numbers in it simulate the change in SMB in a transition from relatively warm to colder conditions. The data in Table 2 and Fig. 8 clearly show that the observed density decrease does not have a noticeable effect on the calculated SMB, especially on the annual SMB. The changes in winter, summer and annual balances (ΔB_w, ΔB_s and ΔB_a, respectively) are in nearly all cases below the estimated accuracy of the SMB values, which is usually assumed to lie within 0.1–0.3 m w.e. (Jansson 1999; Huss *et al*. 2009; Zemp *et al*. 2013). It can also be observed that the differences in results between the two simulated scenarios, *i.e.* density typical of warmer initial conditions as a function of depth, or constant in depth, is irrelevant. The differences in ΔB between both cases can hardly be distinguished.

Of the calculated ΔB results, only those for 2009–10 (not shown in Table 2) had values close to significant (ΔB_a = -0.24 m w.e. for $\rho(H)$ and -0.23 m w.e. for constant ρ), but we decided to exclude these results because the density values for that season were highly anomalous. The standard deviation of the densities of that year was of 60 kg m^{-3}, twice as large as the average of the standard deviations for the remaining years (25 kg m^{-3}). The season 2009–10 was indeed a cold one, with low temperatures even during the summer, so low density values are credible. However, the high standard deviation and the inconsistent behaviour of the density values of the various pits forced us to discard this year's data. Of the remaining years, only 2015–2016 shows ΔB larger than 0.1 m w.e., still within the usual error range of 0.1–0.3 m w.e. This was also a year with both cold winter and cold summer, though not as cold as 2009–10, and with low melt, but in this case the density data were more

Table 2

Calculated surface mass balances (SMBs) using the real densities vs. depth for each individual year and a simulated density, varying with depth and constant with depth, characteristic of the warmer initial temperature conditions for winter and summer, applied to all years during the studied period, and differences between the real and simulated SMBs. Simulated values for 2009–2010 have been excluded because the corresponding density value was removed from the density versus time plot as outlier, but we leave its row in the table to show the SMBs for the year. B_w stays for winter, B_s for summer and B_a for annual SMBs.

SMB (m w.e.)															
Year	Using real $\rho(H)$			Using initial $\rho(H)$						Using initial constant ρ					
	B_w	B_s	B_a	B_w	B_s	B_a	$-\Delta B_w$	$-\Delta B_s$	$-\Delta B_a$	B_w	B_s	B_a	$-\Delta B_w$	$-\Delta B_s$	$-\Delta B_a$
2004–05	0.76	-0.78	-0.02	0.75	-0.77	-0.02	0.01	-0.01	0.00	0.76	-0.77	-0.01	0.00	-0.01	-0.01
2005–06	0.73	-1.32	-0.59	0.73	-1.34	-0.60	0.00	0.02	0.01	0.74	-1.34	-0.60	-0.01	0.02	0.01
2006–07	0.40	-0.80	-0.40	0.41	-0.80	-0.40	-0.01	0.00	0.00	0.41	-0.81	-0.39	-0.01	0.01	-0.01
2007–08	0.80	-0.67	0.13	0.80	-0.69	0.11	0.00	0.02	0.02	0.80	-0.68	0.12	0.00	0.01	0.01
2008–09	0.58	-0.85	-0.27	0.62	-0.89	-0.27	-0.04	0.04	0.00	0.63	-0.90	-0.27	-0.05	0.05	0.00
2009–10	0.74	-0.17	0.57												
2010–11	1.04	-0.63	0.41	1.03	-0.62	0.41	0.01	-0.01	0.00	1.03	-0.61	0.42	0.01	-0.02	-0.01
2011–12	0.63	-0.62	0.01	0.64	-0.62	0.02	-0.01	0.00	-0.01	0.65	-0.62	0.02	-0.02	0.00	-0.01
2012–13	0.82	-0.55	0.27	0.83	-0.56	0.27	-0.01	0.01	0.00	0.83	-0.55	0.28	-0.01	0.00	-0.01
2013–14	0.72	-0.20	0.51	0.79	-0.24	0.54	-0.07	0.04	-0.03	0.79	-0.23	0.53	-0.07	0.03	-0.02
2014–15	1.02	-0.36	0.67	1.12	-0.41	0.71	-0.10	0.05	-0.04	1.11	-0.37	0.74	-0.09	0.01	-0.07
2015–16	0.80	-0.49	0.31	0.83	-0.38	0.45	-0.03	-0.11	-0.14	0.84	-0.37	0.47	-0.04	-0.12	-0.16

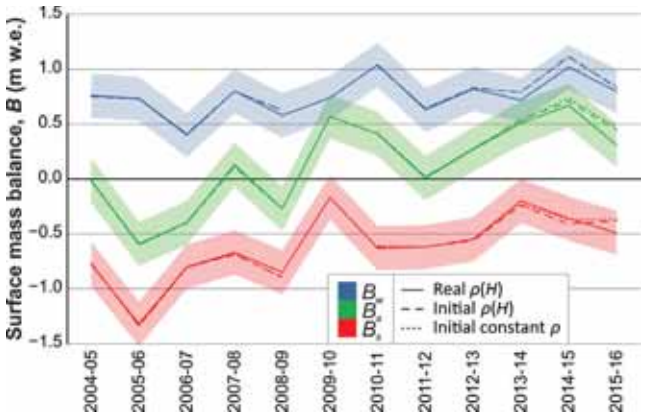

Fig. 8. Winter (B_w), summer (B_s) and annual (B_a) SMBs for all three density scenarios used in Table 2. The shadings indicate the error bars for the SMB values calculated using the real density vs. depth function $\rho(H)$. Modelled values for 2009–10 have been excluded consistently with Table 2.

self-consistent (as compared with those of 2009–10) and the standard deviation acceptable at 31 kg m^{-3}.

Summarizing, although during the period 2004–2016 we observed a density decrease, this has not resulted in a significant change of the calculated SMB. We suggested in the introduction that, although a decrease in winter snow density is expected to produce a less positive winter balance, and a decrease in summer snow density a corresponding less negative, *i.e.* more positive, summer balance, these changes could balance each other. Most of the yearly data shown in Table 2 and Fig. 8 follow this trend, *i.e.* the $-\Delta B_w$ values are predominantly negative, while the $-\Delta B_s$ values are mostly positive, partly balancing each other. A notable exception is year 2015–16, with $-\Delta B_s$ = -0,11, probably due to the high average density for that year in spite of being a cold one. Nevertheless, we have to recognise that the SMB changes implied by the observed density changes are small, even for the winter and summer balance changes, and always below the range of usual errors of SMB data (except 2015–16, in case we consider the lower limit of the error in SMB, 0.1 m w.e.). We also tested what would be the density change required to observe a significant impact on SMB. The results of this experiments show that the density change should be of at least 100 kg m^{-3}, which would need more than 50 years assuming the current density trend.

Although this lack of response of the calculated SMB to the observed density changes could somehow seem disappointing, it can also be considered as a positive outcome. The reason is that it relieves us from the need of detailed and costly (in time) repeated snow-density measurements. If, as a result of precise density measurements based on a few campaigns, we have available some density

www.czasopisma.pan.pl PAN www.journals.pan.pl

value characteristic of our study zone, we can use this value for subsequent SMB campaigns without having to repeat detailed density measurements for each subsequent balance year, because the differences in the calculated SMB values are expected to be very small, and below the usual value of the error in SMB. Moreover, we can use this density either as a function of depth or as a depth-averaged value, since the difference will be irrelevant. Regarding this observation, we note that our study was done using data from glaciers experiencing a sustained (>10 years) episode of cooling of about 0.8°C in 12 years, and therefore our conclusions should not be directly extrapolated to the case of a warming scenario. To gain some insight, we also tested a scenario reversed to our current one in Livingston Island. We considered, under an assumed warming scenario, density conditions starting with our final observed density and ending with our initial one, with a trend reversed to the current one. Then, we used a density typical of the cooler conditions to recalculate the SMB for each individual year and, again, we obtained small changes in SMB, below the usual error range of the SMB calculations. We did not include these results because they did not differ much from those shown in Table 2. Nevertheless, under a scenario of more severe warming the changes in melting, percolation and refreezing within the snowpack could involve more marked density changes that could entail different conclusions. Moreover, an intense warming scenario could also involve changes in the precipitation regime, *e.g.* more abundant rain, that would likely have a further impact on the changes in density of the snowpack.

Conclusions

Summarising the above discussion, the following conclusions can be drawn from our analysis:

1. During the period 2004–2016, the end-of-summer density of the snowpack covering Hurd and Johnsons glaciers has shown a decreasing trend of -1.88 kg m^{-3} a^{-1}, which implies a total decrease in the density of the snow cover of $\Delta\rho$ = -22 kg m^{-3} over the 12-yr study period 2004–2016. This decrease is only poorly statistically significant at p = 0.11, but exceeds in absolute value to all the standard error and the standard deviation of the measurements, and the RMSE of the least-square fit.
2. We attribute the above decrease in density of the snowpack to the recent sustained cooling of about 0.8°C in 12 years (1.0°C in the case of summer temperatures), consistent with the regional cooling for about 15 years since the start of the 21st century, and the expected decrease in surface melting, percolation and refreezing. Changes in liquid precipitation could perhaps have a contribution to the observed density change during winter, although we have no data to support this hypothesis.

www.czasopisma.pan.pl PAN www.journals.pan.pl

3. The observed decrease in density does not have, by itself, a significant impact on the calculated surface mass balance, as the resulting changes are below the range of the usual errors in the estimation of SMB. Consequently, the use of density values typical of the winter and summer seasons for the glacier, when calculating the SMB of subsequent years (instead of the density measured at each particular year), is justified. Moreover, it does not matter whether this typical density is used as a function of depth or as a depth-averaged value, as the implied differences are not significant.
4. The above conclusion can also be applied to reverse conditions, with a density increase of similar magnitude assumed to occur under a warming scenario similar in magnitude (but with opposite sign) to the recent cooling. However, this conclusion cannot be extrapolated to more intense warming conditions, as the associated changes in melting, percolation and refreezing within the snowpack could involve more marked density changes, and more abundant rain could also have a further impact on the changes in the density of the snowpack.
5. Conclusions 3 and 4 suggest that, when only limited input data (*e.g.* snow depth only) are available, a simplified approach for calculating SMB using a constant snow density value might render acceptable results. We recommend that the choice of such a constant value be done taking into account the regional climate conditions and, preferably, based on a local set of measurements of snow density.
6. The cooling conditions that we have analysed are a regional feature. Therefore, a similar density decrease is expected in comparable settings in the Antarctic Peninsula. However, the lack of influence of these density changes on the calculated SMB make them not relevant as concerns to mass budget.

Conclusion 4 suggests the need of carrying out a similar experiment for a glacier with a sufficiently long mass-balance record and that had been subject to an intense warming for a sustained period.

Acknowledgements. — This research was funded by the Spanish State Plan for Research and Development projects CTM2014-56473-R and CTM2017-84441-R. We thank the Spanish Met Office (AEMET) for supplying the meteorological data. Mass balance calculations were made using a modified version, by Ulf Jonsell (Swedish Polar Programme) of a Matlab™ script developed by Rickard Pettersson, Uppsala University, Sweden. Copernicus Sentinel data 2013. We thank the suggestions by two anonymous reviewers, which greatly improved the quality of the manuscript.

www.czasopisma.pan.pl PAN www.journals.pan.pl

References

BADER H. 1954. Sorge's Law of densification of snow on high polar glaciers. *Journal of Glaciology* 2: 319–323.

BAMBER J.L. and KWOK R. 2004. Remote sensing techniques. *In*: Bamber J.L. and Payne A.J. (Eds.): *Mass Balance of the Cryosphere*. Cambridge University Press, Cambridge: 59–113.

BAÑON M. and VASSALLO F. 2015. *AEMET in Antarctica. Climatology and synoptic meteorology in the Spanish meteorological stations in Antarctica*, Ministerio de Agricultura, Alimentación y Medio Ambiente-Agencia Estatal de Meteorología, Madrid: 150 pp. (in Spanish)

BAS 2018. UK Antarctic Surface Meteorology, Reader database (http://www.antarctica.ac.uk/met/READER/), BAS-NERC, doi:10.5285/569d53fb-9b90-47a6-b3ca-26306e696706.

COGLEY J.G., HOCK R., RASMUSSEN L.A., ARENDT A.A., BAUDER A., BRAITHWAITE R.J., JANSSON P., KASER G., MÖLLER M., NICHOLSON L. and ZEMP M. 2011. *Glossary of Glacier Mass Balance and Related Terms*. IHP-VII Technical Documents in Hydrology No. 86, IACS Contribution No. 2, UNESCO-IHP, Paris: 114 pp.

CUFFEY K.M. and PATERSON W.S.B. 2010. *The Physics of Glaciers*, 4th ed. Elsevier, Amsterdam: 704 pp.

DYURGEROV M. 2002. Glacier mass balance and regime: data of measurements and analysis. *Boulder, CO, University of Colorado. Institute of Arctic and Alpine Research. INSTAAR Occasional Paper* 55: 268 pp.

GARDNER A.S., MOHOLDT G., COGLEY J.G., WOUTERS B., ARENDT A.A., WAHR J., BERTHIER E., HOCK R., PFEFFER W.T., KASER G., LIGTENBERG S.R.M., BOLCH T., SHARP M.J., HAGEN J.O., van den BROEKE, M.R. and PAUL F. 2013. A reconciled estimate of glacier contributions to sea level rise: 2003 to 2009. *Science* 340: 852–857.

GONZALEZ S., VASALLO F., RECIO-BLITZ C., GUIJARRO J.A. and RIESCO J. 2018. Atmospheric patterns over the Antarctic Peninsula. *Journal of Climate* 31: 3597–3608.

GRABIEC M., LESZKIEWICZ J., GŁOWACKI P. and JANIA J. 2006. Distribution of snow accumulation on glaciers of Spitsbergen some. *Polish Polar Research* 27: 309–326.

GUIJARRO J.A. 2017. Daily series Homogenization and gridding With Climatol v.3. Proceedings of the 9th Seminar for Homogenization and quality control in climatological databases and 4th conference on spatial interpolation techniques in climatology and meteorology, Budapest, 3–7 April 2017, WCDMP WMO-No. 85: 175–182.

HAGEN J.O. and REEH N. 2004. In situ measurement techniques: land ice. *In*: Bamber J.L. and Payne A.J. (Eds.): *Mass Balance of the Cryosphere*. Cambridge University Press, Cambridge: 11–41.

HANNA E., NAVARRO F.J., PATTYN F., DOMINGUES C., FETTWEIS X., IVINS E.R., NICHOLLS R.J., RITZ C., SMITH B., TULACZYK S., WHITEHOUSE P.L. and ZWALLY H.J. 2013. Ice-sheet mass balance and climate change. *Nature* 498: 51–59.

HUSS M. and HOCK R. 2015. A new model for global glacier change and sea-level rise. *Frontiers in Earth Sciences* 3: 54.

HUSS M., BAUDER A. and FUNK M. 2009. Homogenization of long-term mass-balance time series. *Annals of Glaciology* 50: 198–206.

JANSSON P. 1999. Effect of uncertainties in measured variables on the calculated mass balance of Storglaciären. *Geografiska Annaler A* 81: 633–642.

JONSELL U.Y., NAVARRO F.J., BAÑÓN M., LAPAZARÁN J.J. and OTERO J. 2012. Sensitivity of a distributed temperature-radiation model based on melt index AWS observations and surface energy balance fluxes, Hurd Peninsula glaciers, Livingston Island, Antarctica. *Cryosphere* 6: 539–552.

www.czasopisma.pan.pl PAN www.journals.pan.pl

NAVARRO F.J., OTERO J., MACHERET Y.Y., VASILENKO E.V., LAPAZARAN J.J., AHLSTROM A.P., MACHÍO F. 2009. Radioglaciological studies on Hurd Peninsula glaciers, Livingston Island, Antarctica. *Annals of Glaciology* 50: 17–23.

NAVARRO F., JONSELL U., CORCUERA M.I. and MARTÍN-ESPAÑOL A. 2013. Decelerated mass loss of Hurd and Johnsons Glaciers, Livingston Island, Antarctic Peninsula. *Journal of Glaciology* 59: 115–128.

OLIVA M., NAVARRO F., HRBÁČEK F., HERNANDEZ A., NÝVLT D., PEREIRA P., RUIZ-FERNÁNDEZ J. and TRIGO R. 2016. Recent regional climate cooling on the Antarctic Peninsula and associated impacts on the cryosphere. *Science of the Total Environment* 580: 210–223.

ØSTREM G. and BRUGMAN M. 1991. *Glacier mass-balance measurements: a manual for field and office work* (NHRI Science Report 4) National Hydrology Research Institute, Environment Canada. Saskatoon, Saskatchewan: 224 pp.

STOCKER T.F., QIN D., PLATTNER G.-K., TIGNOR M., ALLEN S.K., BOSCHUNG J., NAUELS A., XIA Y., BEX V. and MIDGLEY P.M. (Eds.) 2013. *Climate Change 2013: The Physical Science Basis*. Contribution of Working Group I to the Fifth Assessment Report of the Intergovernmental Panel on Climate Change. Cambridge University Press, Cambridge, United Kingdom and New York, NY: 1535 pp.

TURNER J., COLWELL S.R., MARSHALL G.J., LACHLAN-COPE T.A., CARLETON A.M., JONES P.D., LAGUN V., REID P.A. and IAGOVKINA S. 2005. Antarctic climate change during last 50 years. *International Journal of Climatology* 25: 279–294.

TURNER J., LU H., WHITE I., KING J.C., PHILLIPS T., HOSKING S.J., BRACEGIRDLE T.J., MARSHALL G.J., MULVANEY R. and DEB P. 2016. Absence of 21st century warming on Antarctic Peninsula consistent with natural variability. *Nature* 535: 411–416.

XIMENIS L. 2001. Dynamics of Johnsons Glacier (Livingston, South Shetland Islands, Antarctica). PhD Thesis, University of Barcelona: 194 pp. (in Catalonian)

XIMENIS L., CALVET J., ENRIQUE J., CORBERA J., FERNANDEZ DE GAMBOA C. and FURDADA G. 1999. The measurement of ice velocity, mass balance and thinning-rate on Johnsons Glacier, Livingston Island, South Shetland Islands, Antarctica. *Acta Geologica Hispanica* 34: 403–409.

ZEMP M., THIBERT E., HUSS M., STUMM D., ROLSTAD DENBY C., NUTH C., NUSSBAUMER S.U., MOHOLDT G., MERCER A., MAYER C., JOERG P.C., JANSSON P., HYNEK B., FISCHER A., ESCHER-VETTER H., ELVEHØY H. and ANDREASSEN L.M. 2013. Reanalysing glacier mass balance measurement series. *The Cryosphere* 7: 1227–1245.

Received 14 March 2018
Accepted 8 October 2018